Macromolecules

pubs.acs.org/Macromolecules Article

Amphiphilic Perfluoropolyether Copolymers for the Effective Removal of Polyfluoroalkyl Substances from Aqueous Environments

Xiao Tan, Jiexi Zhong, Changkui Fu, Huy Dang, Yanxiao Han, Petr Král, Jianhua Guo, Zhiguo Yuan, Hui Peng, Cheng Zhang,* and Andrew K. Whittaker*

Cite This: *Macromolecules* 2021, 54, 3447−3457 Read Online

ACCESS | Metrics & More | Article Recommendations | Supporting Information

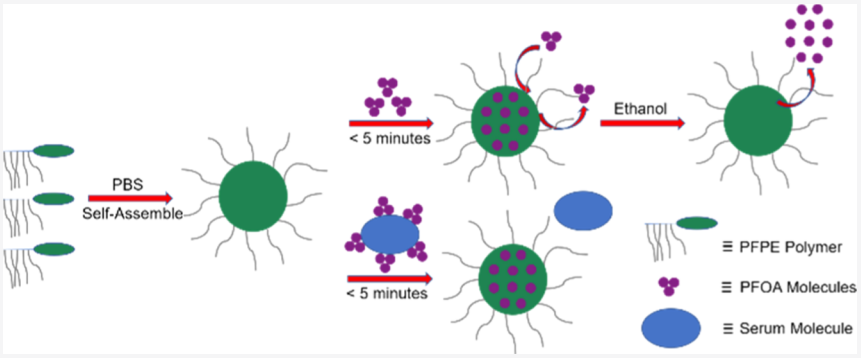

ABSTRACT: Effective removal of per- and polyfluoroalkyl substances (PFAS) from the environment has become a major focus of a number of research groups due to their high stability and persistence in the environment. In this study, we report a fundamental study of the removal of one of the most extensively produced PFAS, perfluorooctanoic acid (PFOA), using amphiphilic perfluoropolyether (PFPE)-containing block copolymers as effective sorbents. The results demonstrate interactions between PFOA and the PFPE blocks and that the extent of sorption is higher for the block copolymer with the shorter poly(oligo(ethylene glycol)methyl ether acrylate) segments. High selectivity of sorption was further confirmed by the addition of 10% (v/v) fetal bovine serum to phosphate-buffered saline. The presence of dissolved proteins and other biomolecules did not interfere with the removal of PFOA from solution. Overall, the results provide important design parameters and a potential platform for preparing efficient sorbents for treating PFAS samples at environmentally relevant concentrations.

INTRODUCTION

Per- and polyfluoroalkyl substances (PFAS) are synthetic compounds widely used in commercial and industrial settings, including as surfactants, lubricants, and foaming agents and in the synthesis of fluoropolymers.[1] PFAS are highly persistent in the environment and several studies have demonstrated bioaccumulation in organisms.[2,3] The levels of accumulation of PFAS can be orders of magnitude times higher than the levels of organochlorine pesticides and dioxin.[4,5] PFAS were also found to display immunotoxicity, neurotoxicity, and mutagenic toxicity on Rana pipiens, rats, and rare minnows, respectively,[6,7] and have accordingly been identified as a class of environmental pollutants with toxicity in multiple organs. Toxicological studies have shown that PFAS primarily causes toxicity by inhibiting the function of the immune system and prohibiting the metabolic activity of the mitochondria, leading to changes in gene expression, death of liver cells, and harm to reproductive cells.[8]

Granulated activated carbon (GAC) with a large surface area is the most widely examined material for the removal of long-chain PFAS, with a removal efficiency of over 90% under optimal conditions.[9,10] However, the removal efficiency was highly affected by numerous factors, such as the presence of inorganic substances in solution, the pH of the solution, and the contact time between sorbate and sorbent.[11,12] Also, the breakthrough of short-chain PFAS for GAC was reported to be rapid, making GAC a challenging technique for long-term PFAS remediation.[13] Membrane filtration, including nanofiltration and reverse osmosis, was also shown to effectively remove PFAS to levels greater that 90%.[14,15] The two filtration methods removed not only both long chains and short chains of PFAS but also other small molecules.[16−18] For instance, inorganic salts were also removed. The nonselectivity nature of the membranes results in the removal of both harmful

Received: January 13, 2021
Revised: March 7, 2021
Published: March 16, 2021

https://dx.doi.org/10.1021/acs.macromol.1c00096
Macromolecules 2021, 54, 3447−3457

substances that are toxic to humans and certain minerals that are essential to human health.[19] Anion exchange, previously used to remove perfluorooctanoic acid (PFOA), perfluorooctanesulfonic acid (PFOS), and perfluorononanoic acid (PFNA), achieves moderate removal efficiency (e.g., 75% for PFOA and 67% for PFNA) depending on the type of resins used.[16] However, adsorption of PFAS by cationic resins was found to be easily influenced by the presence of inorganic anionic ions, as anions competitively bind to active anionic adsorption sites and reduced the maximum adsorption capacity of the resin.[20] Advanced oxidation eliminates micropollutants by introducing nonselective oxidizing species, hydroxyl radicals, and was reported to achieve a removal efficiency toward PFOA and PFNA of less than 10% and a moderate removal efficiency on PFOS (<50%) without removal selectivity.[19,21,22] After oxidation, the contaminants are broken into smaller molecule contaminants, which often require further treatment.[23] The limitations of these conventional methods have prompted the search for novel methods for effective and selective removal of PFAS.

A number of researchers have proposed that fluorinated macromolecules are capable of selective sorption of PFAS as a result of specific hydrophobic interactions.[24−26] Koda et al. reported that microgel star polymers containing perfluoroalkyl segments within the core, prepared using ruthenium-catalyzed living radical polymerization, are able to recognize and separate both water-soluble and water-insoluble PFAS molecules.[27,28] In their initial study,[27] poly(methyl methacrylate) macroinitiators were linked to form a crosslinked core incorporating fluoroalkyl methacrylate monomers. The sorption of perfluorooctane and perfluoromethylcyclohexane was confirmed by careful ^{19}F NMR studies. Subsequently, these authors presented a design capable of removing PFAS from aqueous solutions.[28] In this design, the shell of the core−shell particles consisted of poly(ethylene glycol) (PEG) units and the core incorporated both the fluoroalkyl methacrylate and either quaternized or nonquaternized amine-functionalized methacrylates. Relatively high levels of removal of PFOA and related C8 fluoro-surfactants were reported; however, the inclusion of the amine monomer was required for high levels of removal of the shorter chain perfluorohexanoic acid. Recently, this concept has been extended to particle-embedded hydrogel systems by Quan et al.,[29] who prepared fluorous-core particles by photo-reversible addition−fragmentation chain transfer (RAFT) polymerization of a fluoroalkyl acrylamide with methylene bisacrylamide from a PEG macro-RAFT agent. The authors demonstrated the sorption of a range of fluorinated surfactant molecules by the particles. In order to aid the separation of the fluorous particles, the authors prepared composite hydrogels of crosslinked acrylamide by chain extension from the nanoparticles. The authors were able to demonstrate the removal of PFOA from an aqueous solution and release of PFAS from the particle upon addition of aqueous tetrahydrofuran (THF) or acetone. The combination of a fluorinated monomer and amine-containing monomer was also used by Kumarasamy and co-workers,[30] who prepared a series of crosslinked hydrogels of 2-dimethylaminoethyl methacrylate with a bifunctional perfluoropolyether (PFPE). Importantly, the combination of charged amine groups and fluorocarbon segments allowed removal of a range of PFAS from an aqueous solution collected from a commercial waste treatment plant.

The previous studies have demonstrated the promising potential of partly fluorinated macromolecules for the removal of PFAS in contaminated water. In this study, we chose to examine an alternative class of fluorinated building blocks (i.e., the PFPEs) focusing on the fundamental understanding of interactions between PFOA and PFPE. These chemicals are commercially available in a range of forms with several types of functional end group structures suitable for conjugation and preparation of macroinitiators. A series of block copolymers of PFPE with poly(oligo(ethylene glycol)methyl ether acrylate) (poly(OEGA)) having degrees of polymerization of 5, 10, 20, and 40 were prepared. The sorption of PFOA, one of the most widely used PFAS molecules, was examined in the phosphate-buffered saline (PBS) buffer with or without the presence of fetal bovine serum (FBS). The FBS sample was chosen to examine the effect of additional biomacromolecules in solution on the sorption processes and with a view to potentially incorporate these macromolecules in blood separation devices. Sorption of PFOA was confirmed by detailed ^{19}F NMR and diffusion-ordered spectroscopic measurements, molecular dynamics (MD) simulations, and liquid chromatography−mass spectrometry (LC−MS). The results confirm that this class of aqueous-soluble PFPE-containing block copolymer is a promising sorbent for the effective removal of PFOA from contaminated aqueous solutions.

EXPERIMENTAL SECTION

Materials. The hydroxy-terminated perfluorinated poly(propylene ether) (PFPE-OH, $M_w \sim 1300$ g/mol, CAS number: 1980064-28-5) was purchased from Apollo Scientific Ltd., UK. Oligo(ethylene glycol)methyl ether acrylate (OEGA, M_w = 480 g/mol) purchased from Sigma-Aldrich was passed through basic alumina columns to remove inhibitors before use. The initiator 2,2′-azobis(2-methylpropionitrile) (AIBN) was recrystallized twice from methanol prior to use. The RAFT agent 2-(butylthiocarbonothioylthio)propionic acid (BTPA) was prepared according to a previously reported procedure.[31] Float-A-Lyzer with 500−1000 molecular weight cutoff (MWCO) was purchased from Spectrum Labs and FBS from Thermo Fisher Scientific. All other chemicals were purchased from Sigma-Aldrich and used as received.

Synthesis of the BTPA−PFPE Macro-RAFT Agent. The BTPA−PFPE macro-RAFT agent was prepared by an EDCl/DMAP coupling reaction. In a typical experiment, a solution of *N*-(3-(dimethylamino)propyl)-*N*′-ethylcarbodiimide hydrochloride (0.584 g, 3.05 mmol) in a mixed solvent of dichloromethane (DCM)/trifluorotoluene (TFT) (1:1 v/v) was added slowly to a solution of PFPE-OH (2 g, 1.52 mmol), BTPA (0.435 g, 1.83 mmol), and 4-(dimethylamino)pyridine (DMAP) (0.056 g, 0.46 mmol) in DCM/TFT (1:1 v/v) at 0 °C. The reaction was left at room temperature and stirred for 24 h. The reaction mixture was concentrated and precipitated into a large volume of methanol three times. The BTPA−PFPE macro-RAFT agent, a yellow oil, was obtained by evaporating the methanol at 40 °C under vacuum overnight.

Synthesis of Poly(OEGA)$_x$−PFPE Block Copolymers. Poly(OEGA)$_x$−PFPE block copolymers with different degrees of polymerization of OEGA were synthesized by RAFT polymerization. In a typical experiment, the BTPA−PFPE macro-RAFT agent (1 g, 0.625 mmol), OEGA (1.5 g, 3.125 mmol), and AIBN (20.5 mg, 0.125 mmol) were dissolved in TFT (2.5 mL) in a glass flask with a magnetic stirrer bar and sealed. Argon was introduced to deoxygenate the solution thoroughly for 15 min, and the solution was heated to 70 °C and reacted overnight. Upon completing the reaction, the solution was precipitated into petroleum ether and redissolved in THF three times. The product was obtained by evaporating the solvent at 40 °C under vacuum overnight. Poly(OEGA)$_x$−PFPE copolymers with different degrees of polymerization (x = 5,10, 20, and 40) are referred to as P5, P10, P20, and P40, respectively.

https://dx.doi.org/10.1021/acs.macromol.1c00096
Macromolecules 2021, 54, 3447−3457

Interaction of PFOA with P5, P10, P20, and P40 in PBS. Measurements of sorption of PFOA by the PFPE-containing copolymers were performed as follows: an aliquot of 1 mL of 20 mg/mL polymer solution dissolved in PBS was mixed separately with 0 mg (0 mM, control), 0.33 mg (0.8 mM), 0.64 mg (1.6 mM), 1.33 mg (3.2 mM), and 2.66 mg (6.4 mM) of PFOA in a glass flask with a magnetic stirrer bar for 1 h at room temperature. 450 μL of the solution mixtures with 0 and 3.2 mM PFOA in the presence of the four polymers was mixed with 50 μL of deuterium oxide (D_2O), followed by ^{19}F NMR, ^{19}F NMR DOSY, and dynamic light scattering (DLS) measurements. 3.2 mM PFOA solution without adding a block copolymer was also prepared for ^{19}F NMR and ^{19}F NMR DOSY measurements. The remainder of the solution mixtures was retained for DLS measurements.

Removal Efficiency of PFOA by P5, P10, P20, and P40 in PBS. Polymers with different degrees of polymerization of OEGA were dialyzed against deionized water for 24 h in dialysis tubes with 2000 MWCO. The samples were then fully dried by freeze drying.

For each polymer, 1.5 mL of 20 mg/mL of polymer solution in PBS buffer was prepared. In a typical experiment, the polymer solution was used to dissolve 2 mg of PFOA (3.2 mM). The mixed solution was stirred for 1 h at room temperature, and 1 mL of the solution mixture was transferred into a dialysis device (Float-A-Lyzer) with 500−1000 MWCO and dialyzed against deionized water (100 mL) for 8 h. A control group (3.2 mM PFOA without addition of the polymer) was also studied. A sample of the outer water was collected after dialysis, diluted 50,000 times, and passed through a 0.22 μm polytetrafluoroethylene (PTFE) filter for LC−MS measurement. The removal efficiency was calculated as RE (%) = $[(C_c - C_s)/C_c] \times 100\%$, where C_c and C_s are the concentration of PFOA from the control group and the concentration of PFOA that had passed from the dialysis tube, respectively. The experiments were performed in triplicate.

Release of Bound PFOA from P5. 1 mL of P5 PBS solution (20 mg/mL) was used to dissolve 1.33 mg of PFOA (3.2 mM). The solution was magnetically stirred for 1 h at room temperature, and 400 μL of the solution mixture was taken for ^{19}F NMR and ^{19}F NMR DOSY measurements using a coaxial insert filled with D_2O.

The remainder of the P5-PFOA solution mixture was evaporated by passing nitrogen gas for 6 h to fully dry the sample. Ethanol (~98%, 600 μL) was added to redissolve the sample, and the solution was stirred for 1 h. The ^{19}F NMR spectrum and ^{19}F NMR DOSY were collected in 400 μL of the solution mixture.

Following the measurement of desorption of the PFOA from the copolymer, the ethanol was evaporated under a nitrogen gas flow, and 400 μL of deionized water was added to redissolve the sample. The solution was stirred for 1 h, and ^{19}F NMR measurements were taken.

Sorption of PFOA in PBS in the Presence of FBS. 1 mL of 20 mg/mL of the P5 PBS solution containing 10% (v/v) FBS was used to dissolve 1.33 mg of PFOA (3.2 mM). The solution was magnetically stirred for 1 h at room temperature, followed by ^{19}F NMR and ^{19}F NMR DOSY measurements in 400 μL of the solution mixture. A coaxial insert filled with D_2O was used to lock the magnetic field.

Characterization Methods. *Nuclear Magnetic Resonance (NMR).* ^{1}H NMR spectra of polymer solutions in $CDCl_3$ were acquired on a Bruker AVANCE 400 MHz (9.4 T) spectrometer at 25 °C. A 90° pulse width 14 μs, relaxation delay 1 s, acquisition time 4.1 s, and 32 scans were used in all measurements.

^{19}F NMR spectra were acquired on a Bruker AVANCE 400 MHz spectrometer with either $CDCl_3$ or PBS (with/without 10% FBS) as the solvent. The samples tested in the presence of FBS were prepared by the addition of 10% FBS in the PBS/D_2O (90/10, v/v) solution. Coaxial inserts containing D_2O were used for the measurement of samples in PBS with added FBS. Spectra were measured under the following conditions: 90° pulse width 15 μs, relaxation delay 2 s, acquisition time 0.73 s, and 128 scans.

^{19}F spin−spin relaxation times (T_2) were measured using the Carr−Purcell−Meiboom−Gill pulse sequence at 298 K. The relaxation delay was 2 s, and the number of scans was 64. The relaxation times for the major peaks are reported in this study.

^{19}F NMR DOSY was measured at 298 K under the following conditions: the relaxation delay was 2 s, the diffusion time (Δ) was 0.3 s, and the number of scans was 256.

Size Exclusion Chromatography (SEC). Molecular weights and molecular weight distributions were determined by SEC using a Waters Alliance 2690 separations module equipped with a Waters 2414 refractive index (RI) detector, a Waters 2489 UV/vis detector, a Waters 717 Plus autosampler, and a Waters 1515 isocratic HPLC pump. THF was used as the mobile phase at a flow rate of 1 mL/min. The samples were dissolved in THF at a known concentration (1 mg/mL) and were passed through 0.45 μm PTFE filters before testing. The molecular weight was calculated relative to polystyrene standards.

Dynamic Light Scattering. DLS was conducted on a Nanoseries Zetasizer (Malvern, UK) containing a 2 mW He−Ne laser operating at a wavelength of 633 nm. The scattering angle used was 173°. Each test for the hydrodynamic diameter was repeated three times to provide an average value.

Liquid Chromatography−Mass Spectrometry. A Sciex X500R QTOF system (Sciex Applied Biosystems, MA, USA) coupled to an Exion LC AC liquid chromatograph with C18 column (50 × 2.1 mm, 2.6 μm particle size, Phenomenex, USA) maintained at 40 °C was used for the analysis of PFOA. The mass spectrometer was operated in a negative product ion scan mode of the precursor at m/z 413.0. The fragment at m/z 169.002 ± 0.025 was used for the quantitation of PFOA. The flow rate was set to 0.3 mL/min, and the injection volume was 7 μL. A mobile phase consisting of 0.5 mM aqueous ammonium acetate acid (A) and 0.5 mM aqueous ammonium acetate acid/90% methanol (v/v) (B) was used for LC. The gradient conditions were set at 40% of solvent B for 0.7 min, increased from 40 to 70% within 0.1 min, further increased to 100% at 2 min, and then held for 2.5 min. Thereafter, solvent B was returned to 40% in 0.1 min. The QTOF system was operated in the negative electrospray ionization mode. The spray voltage was set to −4500 V. The temperature of the ionization chamber was set at 420 °C, and the curtain gas was set to 30 psi, while the ion source gases 1 and 2 were both maintained at 50 psi. For TOF MS, the declustering potential (DP) was −60 eV and the collision energy was −10 eV.

MD Simulations. The MD simulations were performed using the NAMD code.[32] The polymers P5−P40 and PFOA were described with the CHARMM general force field.[33,34] The particle mesh Ewald (PME)[35] method was used for the evaluation of long-range Coulombic interactions. The simulations were performed in the NpT ensemble (pressure p = 1 bar, temperature T = 300 K) using Langevin dynamics with a damping constant of 1 ps^{-1} and a time step of 2 fs.

RESULTS AND DISCUSSION

In this study, we introduce a new type of PFPE-containing block copolymer for the removal of an important PFAS, PFOA, from aqueous solutions. The fluorinated block consists of a perfluorinated propylene ether segment and was chain extended with a block of poly(OEGA) using RAFT polymerization. The chemical structure of the PFPE fluorinated block was specifically chosen for several reasons. First and primarily, the high fluorine content will ensure high affinity for aqueous-born fluorinated molecules. Second, the ether units in PFPE imbue the structure with high flexibility compared with that of fluoroalkyl structures (lower cohesive energy density of fluoroethers cf. fluoroalkanes),[36] and we therefore expected, and observed, very rapid rates of sorption of PFOA (<5 min). Finally, the PFPE structure was chosen for the potential to interact with added alcohols through the relatively polar ether moiety to allow isolation of the polymer from the bound PFOA. As previously reported by us, the degree of polymerization (DP) of OEGA affects the aggregation properties in aqueous solution of this class of block copolymer.[37,38] Block copolymers with different DPs of OEGA were prepared

https://dx.doi.org/10.1021/acs.macromol.1c00096
Macromolecules 2021, 54, 3447−3457

(poly(OEGA)$_x$–PFPE, x = 5, 10, 20, and 40) to investigate how the aggregation behavior affects the uptake of PFOA from an aqueous solution. The reaction scheme for the preparation of PFPE-containing block copolymers is shown in Scheme 1.

Scheme 1. Synthesis of PFPE-Containing Block Copolymers with Different DPs of OEGA Block (poly(OEGA)$_x$–PFPE, x = 5, 10, 20, and 40)

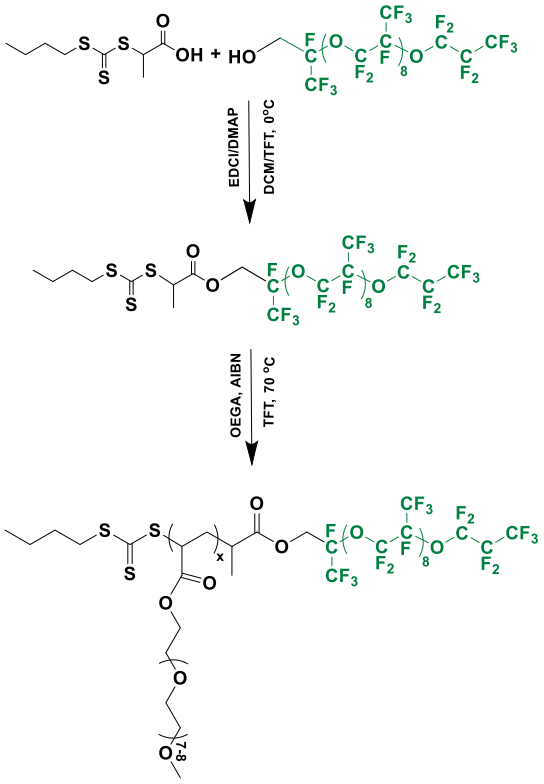

The 2-BTPA–PFPE macro-RAFT agent was prepared by *N*-(3-dimethylaminopropyl)-*N*′-ethylcarbodiimide hydrochloride/4-dimethylaminopyridine coupling. ^{1}H NMR and ^{19}F NMR confirmed that the macro-RAFT agent was successfully synthesized (Figures S1 and S2). A series of poly(OEGA)$_x$–PFPE polymers with different DPs of OEGA were prepared by chain extension. Conversions were determined by ^{1}H NMR of the crude reaction mixtures (see Figure S3 in the Supporting Information for detailed calculations) and were calculated to be 92.3, 93.2, 93.0, and 97.2% for P5, P10, P20, and P40, respectively. The polymers have a low molar mass dispersity ($Đ$ < 1.2) and molecular weights consistent with predicted values (Table 1). Figure 1 shows the ^{1}H and ^{19}F NMR spectra of the poly(OEGA)$_5$–PFPE with the shortest OEGA block (P5, x = 5) after purification for removal of the excess OEGA monomer. All peaks were successfully assigned in both spectra. Figure S4 shows the ^{1}H NMR spectra of the purified P10, P20, and P40, suggesting the successful synthesis of all four polymers.

The poly(OEGA)$_x$–PFPE block copolymers prepared in this study have a tendency to form aggregates in aqueous solution. In previous work, we observed the block copolymer composition, and hence, the aggregation state significantly influences the rate of uptake by breast cancer cells, diffusion within cells and within tumor spheroids.[38] In the current application, we expect that the formation of large aggregates

Table 1. Structural Properties of Poly(OEGA)$_x$–PFPE Polymers

polymer	conversion (%)	$M_{n,NMR}$[a] (g/mol)	$M_{n,SEC}$[b] (g/mol)	$Đ$[b]	PFPE content[c] (wt %)
P5	92.3	3830	3600	1.08	33.9
P10	93.2	6190	3890	1.08	21.0
P20	93.1	10770	5900	1.08	12.1
P40	97.2	20530	7580	1.12	6.3

[a]$M_{n,NMR}$ for the polymers was calculated based on the integrals of the proton peaks H6 and H1. [b]$M_{n,SEC}$ and $Đ$ were acquired by SEC in THF using a RI detector. Polystyrene narrow molecular weight standards were used as the calibrant. [c]The weight percentage of PFPE in the samples.

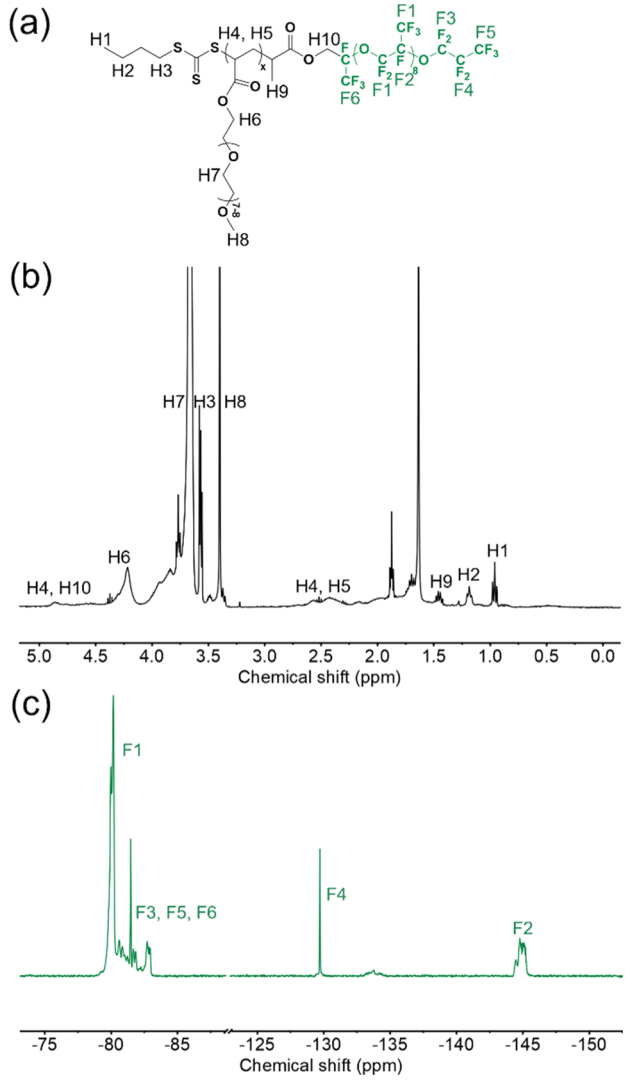

Figure 1. NMR spectra of purified P5 in $CDCl_3$. (a) Chemical structure of P5. (b) ^{1}H and (c) ^{19}F NMR spectra of P5 and numbering scheme used in the NMR spectra.

with PFPE as the core and the extent of exposure of the fluorocarbon to the aqueous environment will strongly affect the interactions with dissolved PFAS molecules. Accordingly, we have measured the hydrodynamic diameter of the four block copolymers in the aqueous solution by DLS (Table S1). As reported in our previous studies, the size of the polymer particles in solution remains constant at around 10 nm apart

https://dx.doi.org/10.1021/acs.macromol.1c00096
Macromolecules 2021, 54, 3447–3457

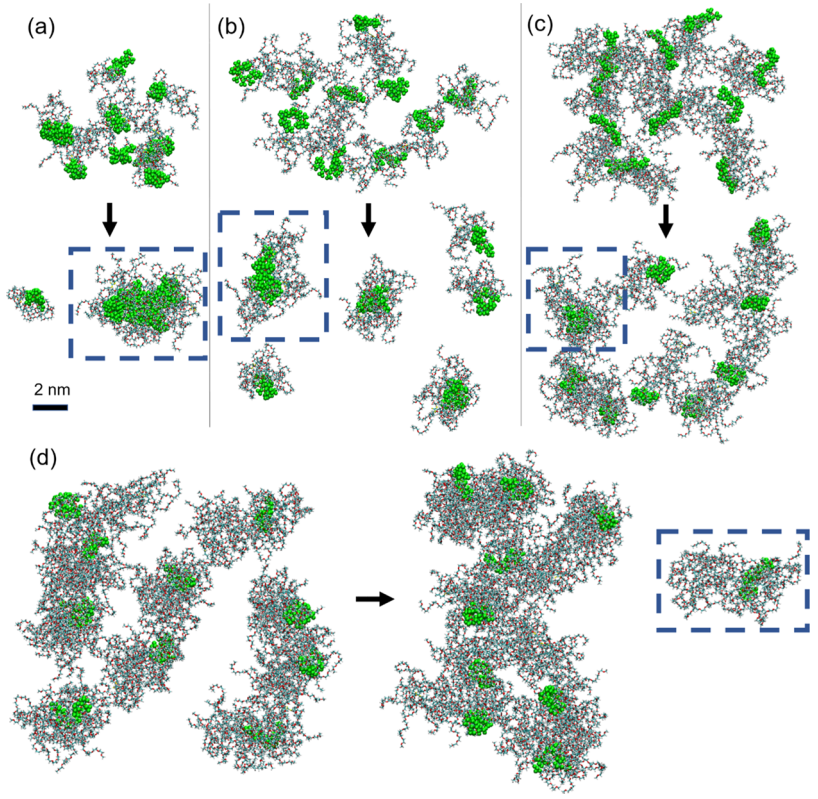

Figure 2. Snapshots from the MD simulations of the self-assembly of the block copolymers in 150 mM NaCl solutions taken at 40 ns (a) P5, (b) P10, (c) P20, and (d) P40. The aggregates of nine P5 chains, three P10, two P20, and the P40 unimer are highlighted in blue dashed boxes. The PFPE segments are shown in green surrounded by the hydrophilic OEGA monomeric units in atomistic detail.

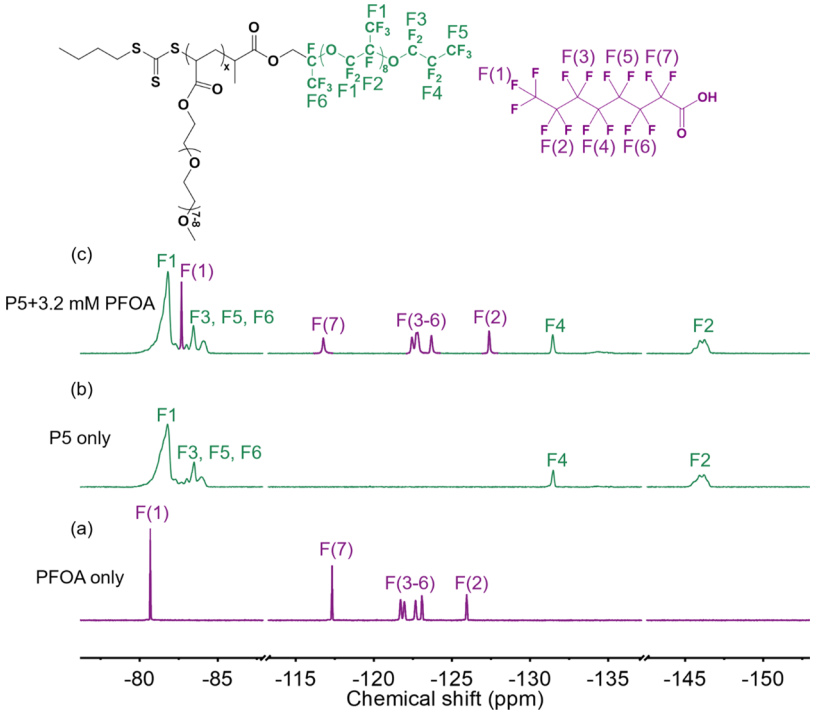

Figure 3. ^{19}F NMR spectra of (a) PFOA, (b) P5, and (c) mixture of PFOA and P5 (90% PBS + 10% D_2O). Peaks F1−F6 are signals from the polymer; peaks F(1)−F(7) are resonances from PFOA. PFOA, 3.2 mM; P5, 20 mg/mL.

from the block copolymer with DP_{OEGA} = 40 (P40), indicating different aggregation behaviors for these four copolymers. The results from ^{19}F DOSY NMR measurements are consistent with the DLS results and are discussed below.

https://dx.doi.org/10.1021/acs.macromol.1c00096
Macromolecules 2021, 54, 3447−3457

Table 2. Diffusion Coefficients and Hydrodynamic Diameters of Poly(OEGA)$_x$−PFPE Block Copolymers with and without the Presence of PFOA in PBS[a]

	D_f [×10^{11} m^2/s, measured for peaks F1 and F(1)]				D_h (nm)			
	P5	P10	P20	P40	P5	P10	P20	P40
polymer only	4.41	4.49	4.36	2.68	11.7	11.5	11.8	19.2
polymer after sorption	4.68	4.69	4.45	2.70	11.0	11.0	11.6	19.1
PFOA only			50.0				1.0	
PFOA after sorption	5.68	6.21	7.26	10.2	9.1	8.3	7.1	5.1
proportion of free PFOA (%)	2.2	3.4	6.2	15.9				

[a]The lowest row shows the proportions of free, unbound PFOA after sorption by the block copolymers in PBS. Polymers, 20 mg/mL; PFOA, 3.2 mM.

MD simulations also demonstrate the different aggregation behavior of the four polymers in ionic solutions. In these simulations, 10 polymer chains of P5, P10, P20, and P40 in 150 mM NaCl solution were placed in separate simulation boxes. The self-assembly of the polymers was simulated for 40 ns to obtain the equilibrium configurations. The results are shown in Figure 2 with the hydrophobic PFPE segments of the copolymers highlighted in green. At 40 ns, multichain aggregates of the copolymers with DP_{OEGA} = 5, 10, and 20 could be observed (blue dashed boxes in Figure 2). To be more specific, the aggregates of P5 comprised nine molecules, the P10 aggregates contained three polymer chains, P20 aggregates had two chains, and P40 did not exhibit multichain aggregation. In summary, the MD simulations show that the aggregation number decreases with increasing size of the hydrophilic OEGA block.

Changes in the NMR spectra are indicative of the interactions between PFOA and the copolymers. The ^{19}F NMR spectrum of PFOA in 90% PBS and 10% D_2O is shown in Figure 3a (3.2 mM). The assignments to the seven resolved peaks in the spectrum are shown in the figure and are consistent with the literature.[39] Narrow, well-resolved peaks are observed in the spectrum as at this concentration PFOA is fully dispersed in the solution, being well below the critical micelle concentration of PFOA (cmc = 25 mM).[40] Note that environmental levels of PFAS may be orders of magnitude small; the higher concentrations used here allow the fundamental NMR study. The ^{19}F NMR spectrum of the copolymer with the lowest OEGA content, P5, is shown in Figure 3b and once again, the assignments are consistent with those reported in the literature.[41−43]

Upon addition of 3.2 mM PFOA to the solution of P5, a number of changes to the NMR spectra become apparent (Figure 3c). The peaks due to the PFPE segments of the block copolymer are largely unaffected by the presence of PFOA in solution, although slight narrowing of the peaks does occur, as discussed below. In addition, all of the resonances due to the fluorinated compound PFOA are shifted. The ^{19}F NMR chemical shift is exquisitely sensitive to the local chemical environment, and the changes in chemical shift can be interpreted as being due to interaction of PFOA with the dissolved polymer and most likely with the PFPE block. Most characteristically, the peak due to the terminal CF_3− of PFOA shifts from −80.7 to −82.7 ppm on mixing with P5. Figure S5 also shows the changes in chemical shifts of PFOA peaks in the presence of P10, P20, and P40 in PBS. The changes in chemical shifts were apparent immediately after mixing the PFOA with the block copolymer, that is, the interactions responsible for the changes were established very rapidly after mixing, agreeing well with the previously reported studies of ionic fluorogel systems.[30]

The second major change in the NMR spectra of PFOA upon mixing with poly(OEGA)$_x$−PFPE is the increased peak width. The dominant mechanism of line broadening in these spectra is homonuclear dipolar coupling, which is averaged by fast librational motion.[44] The increase in line width is evidence of partial restriction of motion of the fluoroalkyl segments of PFOA, and we ascribe this to the sorption of the PFOA into the PFPE domains of the block copolymer assemblies. Similar observations have been reported by others.[28,29] A closer examination of the spectra reveals that the line widths are largest for PFOA interacting with P5, the block copolymer with the lowest OEGA content (Table S2).

^{19}F DOSY NMR is a powerful method for studying the aggregation behavior of polymers in solution.[45] The method provides measurements of self-diffusion coefficients, D_f, for each species giving rise to resolved peaks in the NMR spectrum. The D_f of PFOA in PBS was determined to be 5.0 × 10^{-10} m^2/s, which corresponds to a hydrodynamic diameter of approximately 1 nm, calculated using the Stokes−Einstein equation.[46] As indicated above, the concentration at 3.2 mM is well below the cmc of PFOA,[40] indicating that single-chain molecules of PFOA are presented in solution. The self-diffusion coefficients measured for PFPE block copolymers are listed in Table 2. The calculated hydrodynamic diameters are broadly consistent with the results of DLS measurements discussed above.

After mixing PFOA and the partly fluorinated block copolymer in the PBS solution, the D_f of most species involved changed (Table 2). For block copolymers P5, P10, and P20, the self-diffusion coefficient increased slightly, while for P40, D_f was essentially unchanged. The changes in the self-diffusion coefficients for PFOA were more significant. On interaction with PFPE polymers, the values of D_f for PFOA decreased by at least an order of magnitude (Table 2 and Figure S6). To be more specific, as the proportion of PFPE in the block copolymer decreased (in order from P5 to P40) the difference in self-diffusion coefficient between PFOA and the copolymer increased. The results indicate that during the time scale of the DOSY NMR experiment (the diffusion time, Δ, was 300 ms), PFOA interacted extensively with the block copolymers and diffused at the same rate as a large macromolecule. The results indicate that PFOA was undergoing rapid exchange with the copolymer on the DOSY NMR timescale; this is especially obvious for P40. Therefore, a single averaged diffusion coefficient, weighted by the relative populations of free and bound PFOA, was observed. In the fast exchange regime, the observed diffusion coefficient is equal to the sum of the diffusion coefficients of the "bound" and "free" species,

https://dx.doi.org/10.1021/acs.macromol.1c00096
Macromolecules 2021, 54, 3447−3457

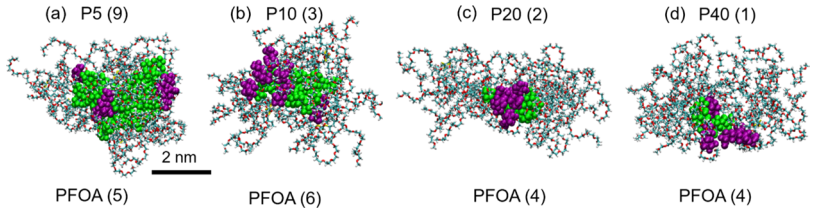

Figure 4. Snapshots of MD simulations of association of PFOA molecules with the self-assembled block copolymers at 25 ns. The PFOA molecules (within 3 Å of PFPE cores) are shown in purple and the PFPE segments in green.

weighted by their number fractions, that is, $D_{observed} = F_{free} \times D_{free} + F_{bound} \times D_{bound}$.[47] The proportion of free (unbound) PFOA was calculated in this manner to be 2.2, 3.4, 6.2, and 15.9% for P5, P10, P20, and P40, respectively (listed in Table 2).

As mentioned above, the diffusion coefficients of P5, P10, and P20 increase upon the addition of 3.2 mM PFOA to the solution, leading to a decreased size, which is consistent with the results measured by DLS (Table S1). As discussed above, MD simulations are an important adjunct to experimental observations.[45,48,49] Additional MD simulations were conducted to support the above NMR observation and to further examine the interaction of PFOA with the block copolymer in solution at the molecular level. In these simulations, 10 molecules of PFOA were added to the simulation box containing the self-assembled copolymer chains (Figure 2), that is, P5 (9 chains), P10 (3 chains), P20 (2 chains), and P40 as single molecule particles. The simulations were performed for 25 ns (Figure 4), until the size of the block copolymer aggregates reached a new equilibrium (Figure S7). PFOA molecules within 3 Å of the PFPE segments were counted and averaged over the last 20 ns. There were five, six, four, and four PFOA molecules attached to the hydrophobic PFPE cores of P5, P10, P20, and P40 aggregates, respectively. This single set of simulations indicates that the highly hydrophobic fluorous segment of the block copolymers interacted strongly with the PFOA molecules in the aqueous solution.

NMR results indicate that the block copolymer, P5, with the smallest fraction of hydrophilic poly(OEGA) block interacts strongly with PFOA in solution. ^{19}F NMR measurements of P5 mixed with varying concentrations of PFOA were conducted (Figure 5). As has been discussed before, the chemical shifts and line widths of the PFOA peaks change in the presence of P5. At all concentrations up to 6.4 mM of PFOA, unique peaks corresponding to PFOA interacting with the block copolymer were observed. Importantly, peaks corresponding to unbound, free PFOA were absent from the spectra even at the highest concentration examined. The NMR spectra also reveal that the width of the peaks arising from the PFPE block of the copolymer becomes progressively narrower upon addition of increasing amounts of PFOA (Table S3). This can only be attributed to plasticization and hence increased librational motion of the PFPE segments, arising from sorption of the low-molecular-weight PFOA. In order to quantify this effect, the transverse (T_2) relaxation times, sensitive to such motions, of the polymer were measured (Figure 6).[48,50] As can be seen,

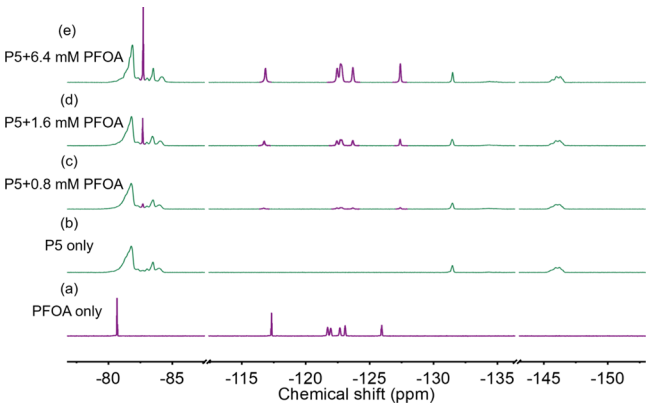

Figure 5. ^{19}F NMR spectra of (a) PFOA, (b) P5, and (c–e) mixture of both at different concentrations of PFOA in PBS at room temperature (90% PBS+ 10% D_2O). PFOA, 0.8–6.4 mM; P5, 20 mg/mL.

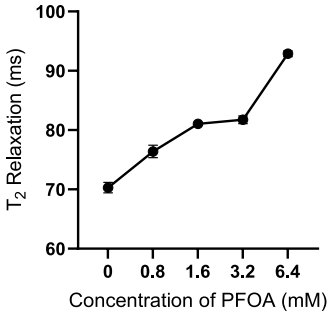

Figure 6. ^{19}F T_2 relaxation times of P5 at 20 mg/mL as a function of concentration of PFOA (measured for the trifluoromethyl group, peak F1). The results are the average of three measurements, and the standard deviation is displayed.

the T_2 relaxation times of peak F1 in the ^{19}F spectrum of the solutions increased significantly upon addition of PFOA. Again, this is clear evidence of extensive interactions upon mixing PFOA with a block copolymer in an aqueous solution.

The utility of poly(OEGA)$_x$–PFPE block copolymers for removing PFOA from aqueous solutions was tested by exposing the copolymer to PFOA and separating the sorbed copolymer particles by dialysis.[28] After exposing the block copolymer to PFOA for 1 h at room temperature, the solution was transferred to a 500–1000 MWCO dialysis tube and dialyzed against distilled water for 8 h. The external solution was sampled and analyzed for PFOA content by LC–MS. The removal efficiencies show that as expected from the characterization experiments described above, the block copolymers with lower OEGA content have higher levels of PFOA removal efficiency at 90 and 87% for P5 and P10, respectively (Figure 7). Under the conditions of an infinite sink employed in this experiment, the copolymers P20 and P40 had removal efficiencies of 55 and 34%, respectively. As revealed by the diffusion NMR experiments, the bound PFOA undergoes fast exchange with free solubilized PFOA, so it is expected that as

https://dx.doi.org/10.1021/acs.macromol.1c00096
Macromolecules 2021, 54, 3447–3457

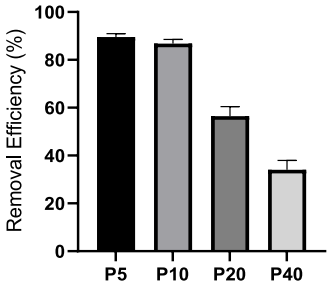

Figure 7. Removal efficiency of 3.2 mM PFOA by P5, P10, P20, and P40 at room temperature (25 °C). The block copolymer concentration was 20 mg/mL. The results are the average of three replicates, and standard deviation is shown.

the diffusion sink becomes very large in the dialysis experiment, PFOA will be desorbed from the block copolymers to a larger extent than in the experiments with a smaller sink described above. In addition, the above experiments were performed based on the same weight of the block copolymer (20 mg/mL); the weight fraction of PFPE in P5 is 34%, while that in P40 is 6%. The dialysis experiments show that the removal efficiency scales well with the PFPE content in solution.

The bound PFOA within the fluorous domains can be simply released by the addition of ethanol. After allowing the sorption of PFOA by the P5 block copolymer to reach equilibrium in PBS, the water was removed by drying under a gas flow, and ethanol was added to disperse the P5 copolymer and the sorbed PFOA. The ^{19}F NMR spectrum of P5 + PFOA in the releasing solvent ethanol is shown in Figure 8c. The

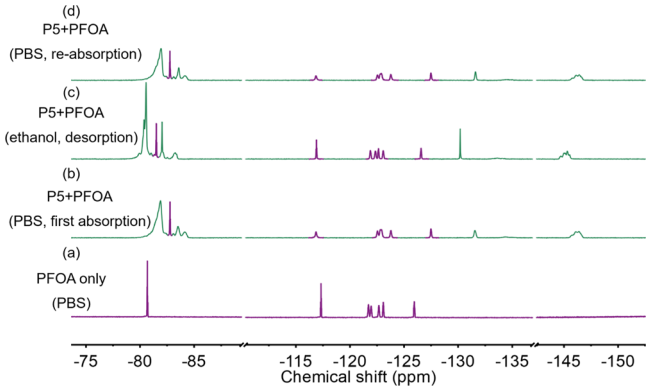

Figure 8. ^{19}F NMR spectra of free, sorbed, released, and resorbed PFOA by P5 in PBS at room temperature. (a) PFOA only; (b) PFOA + P5 in PBS (first sorption); (c) PFOA + P5 in ethanol (desorption); and (d) PFOA + P5 in PBS (resorption). PFOA, 3.2 mM; P5, 20 mg/mL. (a,b,d) were conducted in 90% PBS + 10% D_2O, while (c) was conducted in ethanol with a coaxial insert tube containing D_2O.

chemical shift of the peak due to the terminal CF_3− group of PFOA (−81.4 ppm) became close to the chemical shift of PFOA in ethanol (−81.4 ppm), indicating that the PFOA molecules were in the free unassociated form (Figure S8). The ethanolic solution was then dried, and pure water was added to the mixture. As can be seen in Figure 8d, the ^{19}F NMR spectrum after the addition of ethanol is essentially identical to the original spectrum collected prior to drying and addition of ethanol. ^{19}F NMR DOSY results in Figure S8 further confirm the successful release of PFOA upon addition of ethanol (two sets of different diffusion coefficients, Figure S9a) and resorption in aqueous solution (Figure S9b). These experiments demonstrate that the addition of ethanol results in the release of PFOA from the block copolymer assembly and that in turn replacement of ethanol with water results in the PFOA being resorbed by the block copolymer.

The presence of a dissolved organic species represents a large challenge for effective PFAS remediation.[51−55] In our systems, it is expected that the highly specific nature of the sorption mechanism, being driven by fluorous interactions, can minimize interference from nonfluorinated organic molecules. Therefore, a potential application of the PFPE sorbents reported in this study is the specific removal of PFAS from blood serum. Initially, the interaction of PFOA dispersed in PBS with added FBS was examined. Figure 9c shows the NMR

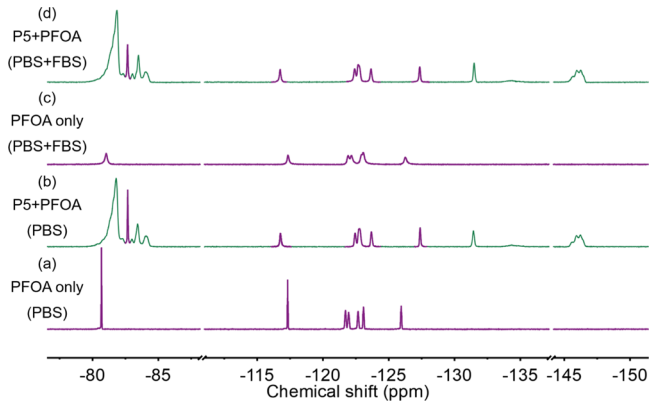

Figure 9. ^{19}F NMR spectra (in D_2O) of PFOA in PBS with/without the presence of FBS, PFOA after sorption by polymer with the presence of serum and polymer only in PBS at room temperature. (a) PFOA only in PBS; (b) PFOA in the presence of P5 in PBS; (c) PFOA only in PBS with the presence of FBS; and (d) PFOA in the presence of P5 in PBS with the presence of FBS. PFOA, 3.2 mM; polymer, 20 mg/mL; FBS, 10% v/v.

spectrum of PFOA dissolved in the PBS + FBS solution. It is notable that compared with the spectrum of PFOA in PBS shown in Figure 9a, the peaks are substantially broader, indicating some level of interaction of the PFOA with serum molecules in solution. Upon addition of P5, the NMR peaks from PFOA shift and appear at chemical shifts identical to the case when PFOA and P5 alone are in the solution (Figure 9d). It is clear that the block copolymer P5 preferentially sorbs the PFOA and is unaffected by the presence of serum molecules.

CONCLUSIONS

This study introduces a new class of block copolymer of PFPE and OEGA that is capable of efficiently interacting with and absorbing PFOA in an aqueous solution. Four polymers with different contents of hydrophilic OEGA and hydrophobic/fluorophilic PFPE were prepared. Consistent with our previous studies, the polymers self-assembled in the aqueous solution to an extent depending on the length of the OEGA block. The polymer with the shortest OEGA blocks, P5, formed aggregates that are most effective in sorbing PFOA from solution with 90% removal efficiency. Diffusion NMR was used to quantify the fraction of free PFOA molecules remaining in solution and undergoing exchange with bound PFOA. Importantly, addition of ethanol resulted in desorption of the PFOA, allowing the block copolymer to be regenerated and reused. The presence of dissolved organic molecules in

https://dx.doi.org/10.1021/acs.macromol.1c00096
Macromolecules 2021, 54, 3447−3457

solution appeared not to interfere with the sorption of PFOA by the block copolymers. These encouraging results demonstrate that PFPE-containing block copolymers can sorb PFOA in various contaminated aqueous solutions. Further investigations will focus on the study of removal efficiency of various PFAS within real water matrices at environmentally relevant concentrations (e.g., contaminated groundwater or wastewater).

■ ASSOCIATED CONTENT

Supporting Information

The Supporting Information is available free of charge at https://pubs.acs.org/doi/10.1021/acs.macromol.1c00096.

Additional ^{1}H NMR and ^{19}F NMR spectra with assignments, DLS profile of poly(OEGA)$_x$–PFPE (x = 5, 10, 20, and 40) block copolymers with or without the presence of PFOA, ^{19}F DOSY NMR characterization of PFOA with the presence of block copolymers, PFOA peak width at half height (in Hz) from ^{19}F NMR spectra, and radius of gyration of aggregated polymers (PDF)

■ AUTHOR INFORMATION

Corresponding Authors

Cheng Zhang − *Australian Institute for Bioengineering and Nanotechnology, The University of Queensland, Brisbane, Queensland 4072, Australia; ARC Centre of Excellence in Convergent Bio-Nano Science and Technology, The University of Queensland, Brisbane, Queensland 4072, Australia;* orcid.org/0000-0002-2722-7497; Email: c.zhang3@uq.edu.au

Andrew K. Whittaker − *Australian Institute for Bioengineering and Nanotechnology, The University of Queensland, Brisbane, Queensland 4072, Australia; ARC Centre of Excellence in Convergent Bio-Nano Science and Technology, The University of Queensland, Brisbane, Queensland 4072, Australia;* orcid.org/0000-0002-1948-8355; Email: a.whittaker@uq.edu.au

Authors

Xiao Tan − *Australian Institute for Bioengineering and Nanotechnology, The University of Queensland, Brisbane, Queensland 4072, Australia; ARC Centre of Excellence in Convergent Bio-Nano Science and Technology, The University of Queensland, Brisbane, Queensland 4072, Australia*

Jiexi Zhong − *Advanced Water Management Centre, The University of Queensland, Brisbane, Queensland 4072, Australia*

Changkui Fu − *Australian Institute for Bioengineering and Nanotechnology, The University of Queensland, Brisbane, Queensland 4072, Australia; ARC Centre of Excellence in Convergent Bio-Nano Science and Technology, The University of Queensland, Brisbane, Queensland 4072, Australia;* orcid.org/0000-0002-2444-607X

Huy Dang − *Department of Chemistry, University of Illinois at Chicago, Chicago, Illinois 60607, United States*

Yanxiao Han − *Department of Chemistry, University of Illinois at Chicago, Chicago, Illinois 60607, United States*

Petr Král − *Department of Chemistry, University of Illinois at Chicago, Chicago, Illinois 60607, United States; Department of Physics and Department of Biopharmaceutical Sciences, University of Illinois at Chicago, Chicago, Illinois 60607, United States;* orcid.org/0000-0003-2992-9027

Jianhua Guo − *Advanced Water Management Centre, The University of Queensland, Brisbane, Queensland 4072, Australia;* orcid.org/0000-0002-4732-9175

Zhiguo Yuan − *Advanced Water Management Centre, The University of Queensland, Brisbane, Queensland 4072, Australia*

Hui Peng − *Australian Institute for Bioengineering and Nanotechnology, The University of Queensland, Brisbane, Queensland 4072, Australia; ARC Centre of Excellence in Convergent Bio-Nano Science and Technology, The University of Queensland, Brisbane, Queensland 4072, Australia*

Complete contact information is available at: https://pubs.acs.org/10.1021/acs.macromol.1c00096

Notes

The authors declare no competing financial interest.

■ ACKNOWLEDGMENTS

The authors acknowledge the Australian Research Council (CE140100036, DP0987407, DP110104299, DP130103774, DP180101221, LE0775684, LE0668517, and LE0882357) and the National Health and Medical Research Council (APP1021759, APP1046831, APP1107723, and APP1158026) for funding this research. C.Z. acknowledges the National Health and Medical Research Council for his Early Career Fellowship (APP1157440). C.F. acknowledges the University of Queensland for a UQ Development Fellowship (UQFEL1831361). The Australian National Fabrication Facility, Queensland Node, and the Queensland Alliance for Environmental Health Sciences (QAEHS) are also acknowledged for access to some items of equipment.

■ REFERENCES

(1) Lau, C. Perfluorinated compounds. *Exp. Suppl.* **2012**, *101*, 47–86.

(2) Haukås, M.; Berger, U.; Hop, H.; Gulliksen, B.; Gabrielsen, G. W. Bioaccumulation of per- and polyfluorinated alkyl substances (PFAS) in selected species from the Barents Sea food web. *Environ. Pollut.* **2007**, *148*, 360–371.

(3) Lesmeister, L.; Lange, F. T.; Breuer, J.; Biegel-Engler, A.; Giese, E.; Scheurer, M. Extending the knowledge about PFAS bioaccumulation factors for agricultural plants–a review. *Sci. Total Environ.* **2021**, *766*, 142640.

(4) Fernández-Sanjuan, M.; Meyer, J.; Damásio, J.; Faria, M.; Barata, C.; Lacorte, S. Screening of perfluorinated chemicals (PFCs) in various aquatic organisms. *Anal. Bioanal. Chem.* **2010**, *398*, 1447–1456.

(5) Thompson, J. Perfluorinated Compounds in the Australian Environment: Sources, Fate and Human Exposure. Ph.D. Dissertation, The University of Queensland, Brisbane, Queensland, 2011.

(6) Giesy, J. P.; Naile, J. E.; Khim, J. S.; Jones, P. D.; Newsted, J. L. Aquatic toxicology of perfluorinated chemicals. *Rev. Environ. Contam. Toxicol.* **2010**, *202*, 1–52.

(7) Stahl, T.; Mattern, D.; Brunn, H. Toxicology of perfluorinated compounds. *Environ. Sci. Eur.* **2011**, *23*, 38.

(8) Webster, G. *Potential Human Health Effects of Perfluorinated Chemicals (PFCs)*; National Collaborating Centre for Environmental Health-NCCEH: Vancouver, Canada, 2010.

(9) Eschauzier, C.; Beerendonk, E.; Scholte-Veenendaal, P.; De Voogt, P. Impact of treatment processes on the removal of perfluoroalkyl acids from the drinking water production chain. *Environ. Sci. Technol.* **2012**, *46*, 1708–1715.

(10) Horst, J.; McDonough, J.; Ross, I.; Dickson, M.; Miles, J.; Hurst, J.; Storch, P. Water Treatment Technologies for PFAS: The Next Generation. *Ground Water Monit. Remed.* **2018**, *38*, 13−23.
(11) Minceva, M.; Fajgar, R.; Markovska, L.; Meshko, V. Comparative Study of Zn^{2+}, Cd^{2+}, and Pb^{2+} Removal From Water Solution Using Natural Clinoptilolitic Zeolite and Commercial Granulated Activated Carbon. Equilibrium of Adsorption. *Separ. Sci. Technol.* **2008**, *43*, 2117−2143.
(12) Aggarwal, D.; Goyal, M.; Bansal, R. C. Adsorption of chromium by activated carbon from aqueous solution. *Carbon* **1999**, *37*, 1989−1997.
(13) Franke, V.; Ullberg, M.; McCleaf, P.; Wålinder, M.; Köhler, S. J.; Ahrens, L. The Price of Really Clean Water: Combining Nanofiltration with Granular Activated Carbon and Anion Exchange Resins for the Removal of Per- And Polyfluoralkyl Substances (PFASs) in Drinking Water Production. *ACS ES&T Water* **2021**, DOI: 10.1021/acsestwater.0c00141.
(14) Flores, C.; Ventura, F.; Martin-Alonso, J.; Caixach, J. Occurrence of perfluorooctane sulfonate (PFOS) and perfluorooctanoate (PFOA) in N.E. Spanish surface waters and their removal in a drinking water treatment plant that combines conventional and advanced treatments in parallel lines. *Sci. Total Environ.* **2013**, *461*−*462*, 618−626.
(15) Tang, C. Y.; Fu, Q. S.; Criddle, C. S.; Leckie, J. O. Effect of flux (transmembrane pressure) and membrane properties on fouling and rejection of reverse osmosis and nanofiltration membranes treating perfluorooctane sulfonate containing wastewater. *Environ. Sci. Technol.* **2007**, *41*, 2008−2014.
(16) Appleman, T. D.; Higgins, C. P.; Quiñones, O.; Vanderford, B. J.; Kolstad, C.; Zeigler-Holady, J. C.; Dickenson, E. R. V. Treatment of poly- and perfluoroalkyl substances in U.S. full-scale water treatment systems. *Water Res.* **2014**, *51*, 246−255.
(17) Eriksson, P. Nanofiltration extends the range of membrane filtration. *Environ. Prog.* **1988**, *7*, 58−62.
(18) Schäfer, A. I.; Fane, A. G.; Waite, T. D. Fouling effects on rejection in the membrane filtration of natural waters. *Desalination* **2000**, *131*, 215−224.
(19) Cummings, L.; Matarazzo, A.; Nelson, N.; Sickels, F.; Storms, C. Recommendation on Perfluorinated Compound Treatment Options for Drinking Water. *New Jersey Drinking Water Quality Institute Treatment Subcommittee Report*: New Jersey, 2015.
(20) Deng, S.; Yu, Q.; Huang, J.; Yu, G. Removal of perfluorooctane sulfonate from wastewater by anion exchange resins: effects of resin properties and solution chemistry. *Water Res.* **2010**, *44*, 5188−5195.
(21) Schröder, H. F.; Meesters, R. J. W. Stability of fluorinated surfactants in advanced oxidation processes−A follow up of degradation products using flow injection-mass spectrometry, liquid chromatography-mass spectrometry and liquid chromatography-multiple stage mass spectrometry. *J. Chromatogr. A* **2005**, *1082*, 110−119.
(22) Schröder, H. F.; José, H. J.; Gebhardt, W.; Moreira, R. F. P. M.; Pinnekamp, J. Biological wastewater treatment followed by physicochemical treatment for the removal of fluorinated surfactants. *Water Sci. Technol.* **2010**, *61*, 3208−3215.
(23) Ribeiro, A. R.; Nunes, O. C.; Pereira, M. F. R.; Silva, A. M. T. An overview on the advanced oxidation processes applied for the treatment of water pollutants defined in the recently launched Directive 2013/39/EU. *Environ. Int.* **2015**, *75*, 33−51.
(24) Xiao, L.; Ling, Y.; Alsbaiee, A.; Li, C.; Helbling, D. E.; Dichtel, W. R. *β*-Cyclodextrin polymer network sequesters perfluorooctanoic acid at environmentally relevant concentrations. *J. Am. Chem. Soc.* **2017**, *139*, 7689−7692.
(25) Lundquist, N. A.; Sweetman, M. J.; Scroggie, K. R.; Worthington, M. J. H.; Esdaile, L. J.; Alboaiji, S. F. K.; Plush, S. E.; Hayball, J. D.; Chalker, J. M. Polymer Supported Carbon for Safe and Effective Remediation of PFOA- and PFOS-Contaminated Water. *ACS Sustain. Chem. Eng.* **2019**, *7*, 11044−11049.
(26) Wang, W.; Xu, Z.; Zhang, X.; Wimmer, A.; Shi, E.; Qin, Y.; Zhao, X.; Zhou, B.; Li, L. Rapid and efficient removal of organic micropollutants from environmental water using a magnetic nanoparticles-attached fluorographene-based sorbent. *Chem. Eng. J.* **2018**, *343*, 61−68.
(27) Koda, Y.; Terashima, T.; Nomura, A.; Ouchi, M.; Sawamoto, M. Fluorinated microgel-core star polymers as fluorous compartments for molecular recognition. *Macromolecules* **2011**, *44*, 4574−4578.
(28) Koda, Y.; Terashima, T.; Sawamoto, M. Fluorous microgel star polymers: selective recognition and separation of polyfluorinated surfactants and compounds in water. *J. Am. Chem. Soc.* **2014**, *136*, 15742−15748.
(29) Quan, Q.; Wen, H.; Han, S.; Wang, Z.; Shao, Z.; Chen, M. Fluorous-Core Nanoparticle-Embedded Hydrogel Synthesized via Tandem Photo-Controlled Radical Polymerization: Facilitating the Separation of Perfluorinated Alkyl Substances from Water. *ACS Appl. Mater. Interfaces* **2020**, *12*, 24319−24327.
(30) Kumarasamy, E.; Manning, I. M.; Collins, L. B.; Coronell, O.; Leibfarth, F. A. Ionic Fluorogels for Remediation of Per- and Polyfluorinated Alkyl Substances from Water. *ACS Cent. Sci.* **2020**, *6*, 487−492.
(31) Ferguson, C. J.; Hughes, R. J.; Nguyen, D.; Pham, B. T. T.; Gilbert, R. G.; Serelis, A. K.; Such, C. H.; Hawkett, B. S. Ab initio emulsion polymerization by RAFT-controlled self-assembly. *Macromolecules* **2005**, *38*, 2191−2204.
(32) Phillips, J. C.; Braun, R.; Wang, W.; Gumbart, J.; Tajkhorshid, E.; Villa, E.; Chipot, C.; Skeel, R. D.; Kalé, L.; Schulten, K. Scalable molecular dynamics with NAMD. *J. Comput. Chem.* **2005**, *26*, 1781−1802.
(33) Vanommeslaeghe, K.; Raman, E. P.; MacKerell, A. D., Jr. Automation of the CHARMM General Force Field (CGenFF) II: Assignment of bonded parameters and partial atomic charges. *J. Chem. Inf. Model.* **2012**, *52*, 3155−3168.
(34) Yu, W.; He, X.; Vanommeslaeghe, K.; MacKerell, A. D., Jr. Extension of the CHARMM General Force Field to Sulfonyl-Containing Compounds and Its Utility in Biomolecular Simulations. *J. Comput. Chem.* **2012**, *33*, 2451−2468.
(35) Darden, T.; York, D.; Pedersen, L. Particle Mesh Ewald - an N.Log(N) Method for Ewald Sums in Large Systems. *J. Chem. Phys.* **1993**, *98*, 10089−10092.
(36) Marchionni, G.; Ajroldi, G.; Righetti, M. C.; Pezzin, G. Molecular-Interactions in Perfluorinated and Hydrogenated Compounds - Linear Paraffins and Ethers. *Macromolecules* **1993**, *26*, 1751−1757.
(37) Zhang, C.; Moonshi, S. S.; Han, Y.; Puttick, S.; Peng, H.; Magoling, B. J. A.; Reid, J. C.; Bernardi, S.; Searles, D. J.; Král, P.; Whittaker, A. K. PFPE-Based Polymeric ^{19}F MRI Agents: A New Class of Contrast Agents with Outstanding Sensitivity. *Macromolecules* **2017**, *50*, 5953−5963.
(38) Zhang, C.; Liu, T.; Wang, W.; Bell, C. A.; Han, Y.; Fu, C.; Peng, H.; Tan, X.; Král, P.; Gaus, K.; Gooding, J. J.; Whittaker, A. K. Tuning of the Aggregation Behavior of Fluorinated Polymeric Nanoparticles for Improved Therapeutic Efficacy. *ACS Nano* **2020**, *14*, 7425−7434.
(39) Han, X.; Snow, T. A.; Kemper, R. A.; Jepson, G. W. Binding of perfluorooctanoic acid to rat and human plasma proteins. *Chem. Res. Toxicol.* **2003**, *16*, 775−781.
(40) Harada, K.; Xu, F.; Ono, K.; Iijima, T.; Koizumi, A. Effects of PFOS and PFOA on L-type Ca^{2+} currents in guinea-pig ventricular myocytes. *Biochem. Biophys. Res. Commun.* **2005**, *329*, 487−494.
(41) Zhang, C.; Li, L.; Han, F. Y.; Yu, X.; Tan, X.; Fu, C.; Xu, Z. P.; Whittaker, A. K. Integrating Fluorinated Polymer and Manganese-Layered Double Hydroxide Nanoparticles as pH-activated ^{19}F MRI Agents for Specific and Sensitive Detection of Breast Cancer. *Small* **2019**, *15*, 1902309.
(42) Zhang, C.; Moonshi, S. S.; Wang, W.; Ta, H. T.; Han, Y.; Han, F. Y.; Peng, H.; Král, P.; Rolfe, B. E.; Gooding, J. J.; Gaus, K.; Whittaker, A. K. High F-Content Perfluoropolyether-Based Nanoparticles for Targeted Detection of Breast Cancer by ^{19}F Magnetic Resonance and Optical Imaging. *ACS Nano* **2018**, *12*, 9162−9176.
(43) Moonshi, S. S.; Zhang, C.; Peng, H.; Puttick, S.; Rose, S.; Fisk, N. M.; Bhakoo, K.; Stringer, B. W.; Qiao, G. G.; Gurr, P. A.;

Whittaker, A. K. A unique ^{19}F MRI agent for the tracking of non phagocytic cells in vivo. *Nanoscale* **2018**, *10*, 8226−8239.
(44) Zhang, C.; Peng, H.; Whittaker, A. K. NMR Investigation of Effect of Dissolved Salts on the Thermoresponsive Behavior of Oligo(ethylene glycol)-Methacrylate-Based Polymers. *J. Polym. Sci., Part A: Polym. Chem.* **2014**, *52*, 2375−2385.
(45) Zhang, C.; Peng, H.; Li, W.; Liu, L.; Puttick, S.; Reid, J.; Bernardi, S.; Searles, D. J.; Zhang, A.; Whittaker, A. K. Conformation Transitions of Thermoresponsive Dendronized Polymers across the Lower Critical Solution Temperature. *Macromolecules* **2016**, *49*, 900−908.
(46) Zhang, C.; Sanchez, R. J. P.; Fu, C.; Clayden-Zabik, R.; Peng, H.; Kempe, K.; Whittaker, A. K. Importance of Thermally Induced Aggregation on ^{19}F Magnetic Resonance Imaging of Perfluoropolyether-Based Comb-Shaped Poly(2-oxazoline)s. *Biomacromolecules* **2019**, *20*, 365−374.
(47) Truong, N. P.; Zhang, C.; Nguyen, T. A. H.; Anastasaki, A.; Schulze, M. W.; Quinn, J. F.; Whittaker, A. K.; Hawker, C. J.; Whittaker, M. R.; Davis, T. P. Overcoming Surfactant-Induced Morphology Instability of Noncrosslinked Diblock Copolymer Nano-Objects Obtained by RAFT Emulsion Polymerization. *ACS Macro Lett.* **2018**, *7*, 159−165.
(48) Zhang, C.; Moonshi, S. S.; Peng, H.; Puttick, S.; Reid, J.; Bernardi, S.; Searles, D. J.; Whittaker, A. K. Ion-Responsive ^{19}F MRI Contrast Agents for the Detection of Cancer Cells. *ACS Sens.* **2016**, *1*, 757−765.
(49) Zhang, C.; Peng, H.; Puttick, S.; Reid, J.; Bernardi, S.; Searles, D. J.; Whittaker, A. K. Conformation of Hydrophobically Modified Thermoresponsive Poly(OEGMA-Co-TFEA) across the LCST Revealed by NMR and Molecular Dynamics Studies. *Macromolecules* **2015**, *48*, 3310−3317.
(50) Zhang, C.; Kim, D. S.; Lawrence, J.; Hawker, C. J.; Whittaker, A. K. Elucidating the Impact of Molecular Structure on the ^{19}F NMR Dynamics and MRI Performance of Fluorinated Oligomers. *ACS Macro Lett.* **2018**, *7*, 921−926.
(51) Kookana, R. S.; Baskaran, S.; Naidu, R. Pesticide fate and behaviour in Australian soils in relation to contamination and management of soil and water: a review. *Aust. J. Soil Res.* **1998**, *36*, 715−764.
(52) Mackay, D. M.; Roberts, P. V.; Cherry, J. A. Transport of organic contaminants in groundwater. *Environ. Sci. Technol.* **1985**, *19*, 384−392.
(53) Pruell, R. J.; Rubinstein, N. I.; Taplin, B. K.; Livolsi, J. A.; Bowen, R. D. Accumulation of Polychlorinated Organic Contaminants from Sediment by 3 Benthic Marine Species. *Arch. Environ. Contam. Toxicol.* **1993**, *24*, 290−297.
(54) Perelo, L. W. Review: In situ and bioremediation of organic pollutants in aquatic sediments. *J. Hazard. Mater.* **2010**, *177*, 81−89.
(55) Schwarzenbach, R. P.; Escher, B. I.; Fenner, K.; Hofstetter, T. B.; Johnson, C. A.; von Gunten, U.; Wehrli, B. The challenge of micropollutants in aquatic systems. *Science* **2006**, *313*, 1072−1077.

https://dx.doi.org/10.1021/acs.macromol.1c00096
Macromolecules 2021, 54, 3447−3457